Chondrocytes respond to an altered heparan sulfate composition with distinct changes of heparan sulfate structure and increased levels of chondroitin sulfate

Velina Bachvarova [a], Tabea Dierker [b], Jeffrey Esko [c], Daniel Hoffmann [d], Lena Kjellen [b] and Andrea Vortkamp [a]

***a* - Department of Developmental Biology, Faculty of Biology and Centre for Medical Biotechnology,** *University of Duisburg-Essen, Universitätsstr 1-5, Essen 45117, Germany*

***b* - Department of Medical Biochemistry and Microbiology, and Science for Life Laboratory,** *Uppsala University, Box 582, Uppsala 75123, Sweden*

***c* - Department of Cellular and Molecular Medicine,** *UCSD, United States*

***d* - Department of Bioinformatics and Computational Biophysics, Faculty of Biology and Centre for Medical Biotechnology,** *University of Duisburg-Essen, Germany*

Corresponding authors.
velina.bachvarova@uni-due.de, tabea.dierker@imbim.uu.se, jesko@ucsd.edu, daniel.hoffmann@uni-due.de, lena.kjellen@imbim.uu.se, andrea.vortkamp@uni-due.de.
https://doi.org/10.1016/j.matbio.2020.03.006

Abstract

Heparan sulfate (HS) regulates the activity of many signaling molecules critical for the development of endochondral bones. Even so, mice with a genetically altered HS metabolism display a relatively mild skeletal phenotype compared to the defects observed in other tissues and organs pointing to a reduced HS dependency of growth-factor signaling in chondrocytes. To understand this difference, we have investigated the glycosaminoglycan (GAG) composition in two mouse lines that produce either reduced levels of HS (*Ext1*$^{gt/gt}$ mice) or HS lacking 2-*O*-sulfation (*Hs2st1*$^{-/-}$ mice). Analysis by RPIP-HPLC revealed an increased level of sulfated disaccarides not affected by the mutation in both mouse lines indicating that chondrocytes attempt to restore a critical level of sulfation. In addition, in both mutant lines we also detected significantly elevated levels of CS. Size exclusion chromatography further demonstrated that *Ext1*$^{gt/gt}$ mutants produce more but shorter CS chains, while the CS chains produced by (*Hs2st1*$^{-/-}$ mice) mutants are of similar length to that of wild type littermates indicating that chondrocytes produce more rather than longer CS chains. Expression analysis revealed an upregulation of aggrecan, which likely carries most of the additionally produced CS. Together the results of this study demonstrate for the first time that not only a reduced HS synthesis but also an altered HS structure leads to increased levels of CS in mammalian tissues. Furthermore, as chondrocytes produce 100-fold more CS than HS the increased CS levels point to an active, precursor-independent mechanism that senses the quality of HS in a vast excess of CS. Interestingly, reducing the level of cell surface CS by chondroitinase treatment leads to reduced Bmp2 induced Smad1/5/9 phosphorylation. In addition, Erk phosphorylation is increased independent of Fgf18 treatment indicating that both, HS and CS, affect growth factor signaling in chondrocytes in distinct manners.

Introduction

Heparan sulfate (HS) carrying proteoglycans (HSPGs) are main components of the extracellular matrix (ECM). They are associated with the cell surface of virtually all vertebrate cells regulating the distribution and activity of many extracellular proteins. HSPGs consist of core proteins to which one or more HS chains are attached. The assembly of the HS chains takes place in the Golgi apparatus. It is commenced by the synthesis of a tetrasaccharide linkage region consisting of one xylose, two galactose, and

one D-glucuronic acid (GlcA) attached to a specific serine residue of the core protein. Subsequently, the glycosyltransferase Extl3 transfers an *N*-acetylglucosamine (GlcNAc) to the tetrasaccharide, followed by the addition of alternating units of GlcA and GlcNAc by the glycosyltransferases Ext1 and Ext2, which act in heteromeric complexes. In parallel, several sulfotransferases and one epimerase modify the growing chain. The first step is the deacetylation and subsequent *N*-sulfation of GlcNAc (GlcNS) by *N*-deacetylase/*N*-sulfotransferases (Ndst1-4) in distinct regions of the HS chains. A subset of GlcA residues, mainly in these *N*-sulfated regions, is then epimerized to iduronic acid (IdoA) by the D-glucuronyl-C5-epimerase (Glce). Further modifications include the addition of sulfate groups to the 2-*O*-position of IdoA and the 3-*O*- and 6-*O*-positions of GlcNAc and GlcNS by different *O*-sulfotransferases. The modifying enzymes show overlapping but distinct expression patterns in different tissues and developmental stages, generating cell-type-specific sulfation signatures. Extensive analyses of HS structure and function have shown that the specific pattern of sulfation determines the binding affinity of HS to growth factors, cytokines and other extracellular proteins, thereby modulating their distribution and activity in the extracellular space [1–4].

Analysis of different mouse models revealed that inactivating mutations of *Ext1* or *Ext2* are gastrula lethal due to impaired mesoderm formation [5,6]. Furthermore, inactivation of individual modifying enzymes results in severe developmental defects in various organs supporting the importance of the HS structure for tissue development and maintenance [7,8].

Most of the bones of the vertebrate body are formed by endochondral ossification, a complex process during which a cartilage template is successively replaced by bone tissue. During endochondral ossification, chondrocytes undergo a highly organized differentiation sequence from proliferating into hypertrophic chondrocytes, which is regulated by the complex interaction of numerous signaling systems including Fgf, Hedgehog, Wnt and Bmp signaling [9–11].

In chondrocytes, a reduction of *Ext1* expression to 3–5% in the hypomorphic $Ext1^{gt/gt}$ mutant [12] leads to severely delayed chondrocyte differentiation due to increased Indian hedgehog (Ihh) signaling [13]. However, although complete deletion of *Ext1* is gastrula lethal, inactivation in the developing limb mesenchyme using *Prx1*-Cre as a driver results in severely reduced and malformed but distinctly developed limb structures [14]. Similarly, while severely affecting different organs, mutations in many modifying enzymes lead to only mild alterations in the endochondral skeleton. For example, loss of Glce or the HS 2-*O*-sulfotransferase 1 (Hs2st1) is lethal due to kidney agenesis ([15–17]), and Ndst1 mutants display multiple, severe developmental defects including holoprosencephaly, craniofacial malformations, neural tube closure and eye defects [18,19]. Nevertheless, despite the fact that endochondral ossification is under the control of similar pathways as those affected in the various mutants, skeleton development is not severely disturbed [20]. This leads to the question if signaling in chondrocytes is less dependent on HS. Alternatively, chondrocytes may have developed specific mechanisms to compensate for an altered HS structure.

One specific feature of chondrocytes is the abundant and complex ECM, which they produce. This matrix consists mainly of the nonsulfated glycosaminoglycan (GAG) hyaluronan, collagens and other structural proteins, and is particularly rich in chondroitin sulfate (CS) carrying proteoglycans (PGs). CS is structurally closely related to HS but contains *N*-acetylgalactosamine (GalNAc) instead of GlcNAc. Like HS, CS is synthesized in the Golgi apparatus. Interestingly, the same tetrasaccharide linkage region that is used to initiate the HS chains also serves as a primer for the biosynthesis of CS. Subsequently, CS-specific *N*-acetylgalactosaminyltransferases (CSGalNAcT1 and CSGalNAcT2) catalyze the addition of GalNAc to the linkage tetrasaccharide, thereby directing the synthesis towards a CS chain. The chain is then elongated by a complex of at least two chondroitin sulfate synthetases (ChSy1-3, and chondroitin polymerization factor (ChPF)). Several CS-specific sulfotransferases add sulfate groups to the 4-*O* (Chst11-13) and 6-*O* (Chst3, Chst15) position of GalNAc, and the 2-*O*-position (uronyl 2-*O*-sulfotransferase, Ust) of GlcA. In addition, epimerization of GlcA to IdoA by two CS-specific glucuronyl C5-epimerases (Dse1-2) transforms the molecule into the stereoisomer dermatan sulfate (DS) [21,22].

In chondrocytes, some CS-carrying PGs like chondroitin sulfate proteoglycan 4 (Cspg4/NG2) and betaglycan [23,24], are associated with the cell surface, while the vast amount of CS is bound to aggrecan and secreted into the interterritorial ECM. Together with hyaluronan, aggrecan-bound CS is responsible for the hydrostatic characteristics and compressive resistance of the cartilage tissue [25,26]. Besides its structural function, CS may also modulate cell signaling since it has recently been shown to bind to different growth factors like Ihh, Fgfs, Vegf and Wnts, although with different affinities compared to HS [27-34].

Based on its structural and biochemical characteristics, CS is a good candidate to substitute for an altered HS structure in chondrocytes. In this study, we thus asked whether alterations in the HS composition might trigger compensatory changes in CS level or structure. We have focused on two mouse strains carrying either severely reduced HS levels ($Ext1^{gt/gt}$) or an altered HS-sulfation pattern ($Hs2st1^{-/-}$). Interestingly, CS levels were increased in both mutants, while the CS disaccharide composition was unaffected. Distinct changes in HS and CS chain length, were also found in both mutants.

Analysis of Fgf and Bmp signaling after CS removal pointed to an important role of CS in regulating growth factor signaling in chondrocytes.

Results

Chondrocytes compensate HS deficiency by an increased CS content

To investigate how the GAG biosynthetic machinery in chondrocytes responds to an altered HS structure, we analyzed the GAG composition in mice carrying a hypomorphic allele of *Ext1* (*Ext1*$^{gt/gt}$) [12,13]. As reported before, mouse embryonic fibroblasts (MEF) of these mutants produce about 20% of HS compared to wild type MEFs [35]. To confirm that HS levels are also reduced in *Ext1*$^{gt/gt}$ chondrocytes, we analyzed the HS distribution in E15.5 forelimb sections using the HS-specific antibodies 10E4 and 3G10 (Fig. 1) [36]. While 10E4 recognizes common *N*-sulfated domains in HS and can therefore be used to assess the total HS amount, the 3G10 antibody detects a neoepitope (ΔHS) generated by heparitinase digestion, providing information about the number of HS chains. Analysis of the immunofluorescence signal on E15.5 forelimb sections revealed reduced total levels of HS in E*xt1*$^{gt/gt}$ mutants, while the number of chains seemed not to be altered (Fig. 1(A) and (C)).

To identify potential alterations in the level of CS, we used antibodies specific to the CS neoepitopes ΔDi-0S (1B5), ΔDi-4S (2B6) and ΔDi-6S (3B3) generated by chondroitinase ABC (CSase ABC) digestion [37,38]. Quantification of the immunofluorescence intensity showed increased levels of each CS neoepitope in *Ext1*$^{gt/gt}$ chondrocytes indicating that the reduced HS levels lead to an increase in the number of CS chains in chondrocytes (Fig. 1(B) and (C)).

To verify these findings, we purified sulfated GAGs from E15.5 mouse skeletons, which at this stage mostly consist of cartilage. We first analyzed the total GAG amount using the carbazole assay [39,40] and found an increase by 65% in *Ext*$^{gt/gt}$ mutants compared to wild type littermates (Fig. 1 (D)). We next determined the amount and disaccharide composition of HS and CS by RPIP-HPLC (Fig. 2). In agreement with earlier studies, the amount of total HS in *Ext*$^{gt/gt}$ mutants was reduced to 20% of control littermates, while the degree of sulfation was not considerably changed (Fig. 2(A) and (B)). Detailed disaccharide analysis revealed an increase in total 6-*O*-sulfation, mostly found on *N*-sulfated disaccharides and, consequently, fewer mono *N*-sulfated disaccharides. Nevertheless, similar to *Ext*$^{gt/gt}$ MEFs, it is mainly the amount of HS, not its composition that is altered in *Ext1*$^{gt/gt}$ chondrocytes (Fig. 2(C)).

Analysis of CS disaccharides revealed a 70% increase in the total level of CS compared to littermate controls, while the relative degree of sulfation and the disaccharide composition were not altered (Fig. 2(D)−(F)). Chondrocytes thus seem to increase the level of CS but maintain a wild type sulfation state in response to reduced HS levels. Interestingly, as HS represents only 1% of sulfated GAGs in chondrocytes (compare Fig. 2(A) and (D)), each pmol HS is replaced by nearly 100 pmol CS, resulting in the observed increase in total GAGs.

Ext1$^{gt/gt}$ synthesize more low molecular weight CS chains

Altered GAG levels could be due to changes in the number of chains, their length or a combination of both. To investigate whether the length of the HS and CS chains is altered in mutant chondrocytes, we isolated ^{35}S-labeled GAGs from the cell lysate of differentiated primary chondrocyte cultures incubated in the presence of [^{35}S]sulfate. In addition, we analyzed the GAGs attached to PGs released into the cell-culture medium, which represent the PGs of the interterritorial ECM of chondrocytes.

The ^{35}S-labeled macromolecules were recovered from the cell lysate and culture medium using DEAE ion-exchange chromatography followed by size exclusion chromatography [41]. While the high molecular weight PGs of the cell lysates eluted in a single peak, the PGs of the culture medium contained two populations of different size (CM I and CM II), which were analyzed separately (Supplementary Fig. 1). Comparing the amounts of ^{35}S-labeled macromolecules detected in the cell lysate and the culture medium revealed that in wild type chondrocytes the vast majority of GAGs (83%) is secreted, likely reflecting the high aggrecan content of the interterritorial ECM (data not shown).

After release from the core proteins, the size of total GAG, HS and CS chains was assessed by size exclusion chromatography before and after chondroitinase ABC digestion and nitrous acid depolymerization, respectively. In wild type chondrocytes similar amounts of labeled HS and CS are present on the cell surface with CS chains representing the GAG population of higher apparent molecular weight (Supplementary Fig. 2(A), Table 1). As shown before for MEFs [35], the relative amounts and length of the HS chains were reduced in the cell lysate of *Ext*$^{gt/gt}$ chondrocytes (Fig. 3(A), Supplementary Fig. 2(B), Table 1). Surprisingly, mutant CS showed a distinct increase in low molecular weight chains in *Ext*$^{gt/gt}$ mice (Fig. 3(B), Supplementary Fig. 2(B)).

Similar to the cell lysate, the amount of ^{35}S-labeled HS recovered from the culture medium of *Ext1*$^{gt/gt}$ chondrocytes was reduced (from about 9% to 4%, Table 1) and due to its low amount was not further analyzed. The CS chains released into the

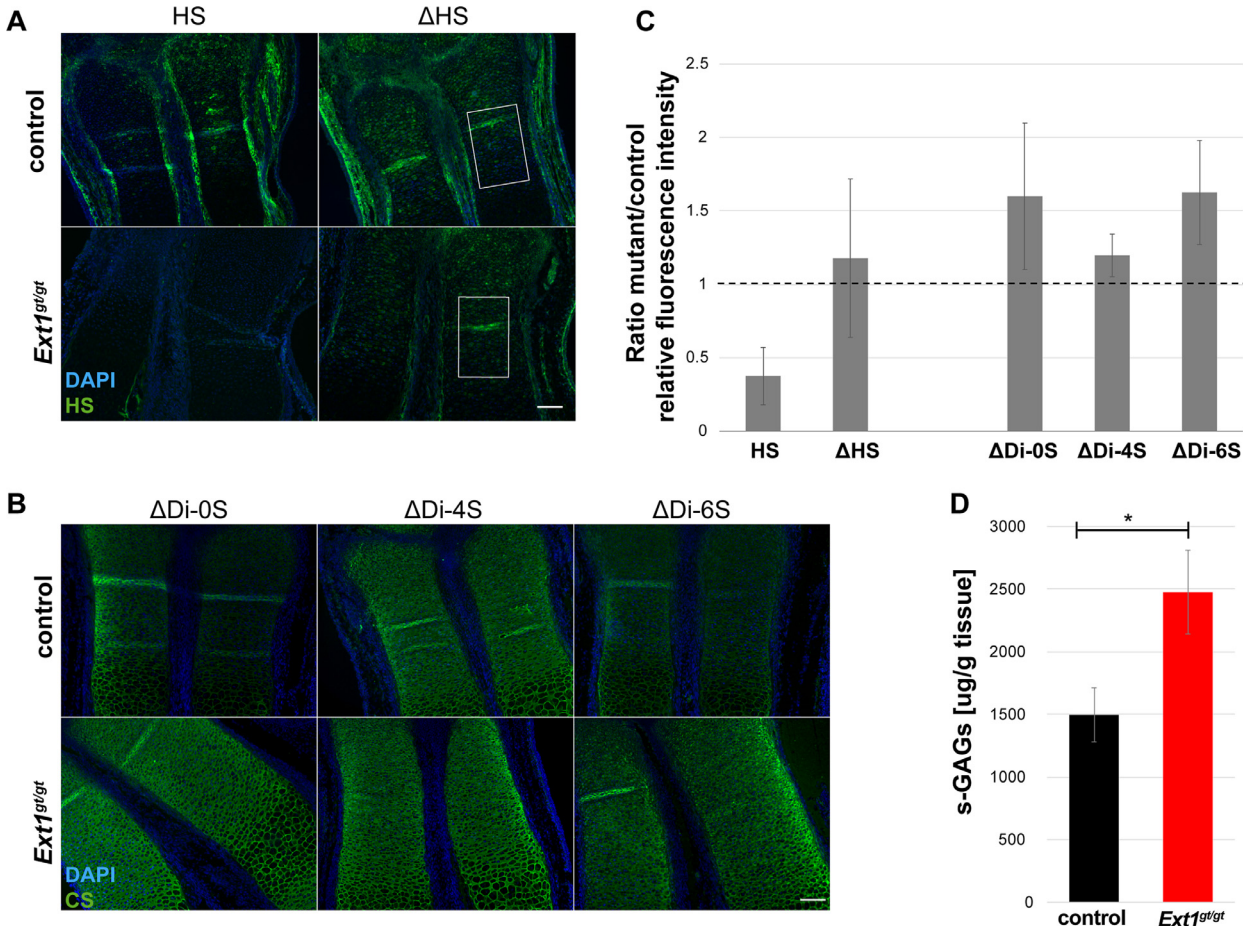

Fig. 1. Increased CS levels in HS-deficient embryonic cartilage. Forelimb sections of E15.5 *Ext1*$^{gt/gt}$ and control embryos were probed with monoclonal antibodies (*green*) recognizing native HS chains (HS), the HS neoepitope (ΔHS) (A) and the CS neoepitopes ΔDi-0S, ΔDi-4S, ΔDi-6S (B). Sections were counterstained with DAPI (*blue*). (A) and (C) While the amount of total HS was reduced (HS) in *Ext1*$^{gt/gt}$ forelimb sections, no alterations in the number of HS primers (ΔHS) could be detected. (B) and (C) CS neoepitopes were increased in *Ext1*$^{gt/gt}$ cartilage. (C) The intensity of the fluorescence signal in the zone of columnar chondrocytes (white rectangles in A) was quantified and normalized to the nuclear DAPI signal. Data are mean values ± s.e.m. relative to the control sample set to 1. $n = 3$. (D) Quantification of sulfated GAGs of E15.5 *Ext1*$^{gt/gt}$ and control skeletal element by carbazole assay showed an increase in the GAG amount of 65% in *Ext1*$^{gt/gt}$ embryonic skeletons compared to control littermates. Values are normalized to tissue dry weight and shown as mean ± s.e.m. $n = 4$. Statistical significance was calculated by unpaired, two-tailed Student's *t*-test. * $p<0.05$. Scale bars: 100 μm (A) and (B). (For interpretation of the references to color in this figure legend, the reader is referred to the web version of this article.)

medium showed a slight but reproducible reduction in length compared to wild type controls (Fig. 3(C) and (D)). In summary, these experiments strongly indicate that the increased level of CS in *Ext1*$^{gt/gt}$ chondrocytes is due to an increased production of shorter chains.

CS levels are increased in undifferentiated limb mesenchymal cells of *Ext1*$^{gt/gt}$ mutants

As described above, chondrocytes are a unique cell type producing particularly high levels of CS [23]. To address the question whether the observed changes in CS level and chain length are a specific feature of this cell type, we analyzed the GAGs of undifferentiated limb mesenchymal cells (LMCs) of wild type and *Ext1*$^{gt/gt}$ mice after metabolic labeling with [^{35}S]sulfate (Fig. 4). In contrast to chondrocytes, which contain similar levels of ^{35}S-labeled HS and CS on the cell surface, wild type LMCs are mainly decorated with HS (Supplementary Figure 2C). Comparing the GAG composition of wild type and mutant cells revealed the expected reduced HS levels in *Ext1*$^{gt/gt}$ cells (Fig. 4(A), Supplementary Fig. 2 (C) and (D)). Importantly, since similar amounts of labeled GAGs were isolated from mutant and control cells (data not shown), ^{35}S-labeled CS had replaced the lost HS in *Ext1*$^{gt/gt}$ LMCs (Fig. 4(B), Supplementary Fig. 2(D)). Similar to chondrocytes, the length of the HS chains was reduced in the mutant, while the

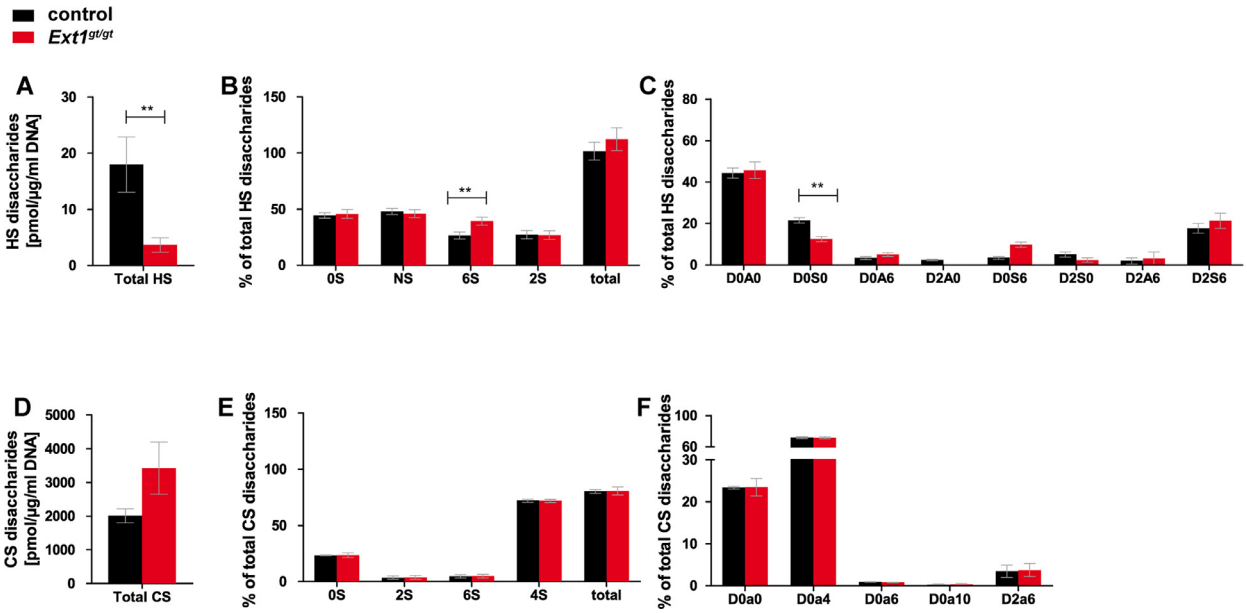

Fig. 2. *Ext1*$^{gt/gt}$ chondrocytes carry increased levels of CS. The amount (A, D) and disaccharide composition of HS (B, C) and CS (E, F) isolated from E15.5 *Ext1*$^{gt/gt}$ (*red*) and control (*black*) skeletal elements, were analyzed by RPIP-HPLC. (A, D) The total amount of HS was reduced to 20% in *Ext1*$^{gt/gt}$ mutants, while the CS level was increased by 70%. (B, C) HS 6-*O*-sulfation was increased in *Ext1*$^{gt/gt}$ chondrocytes, while the CS sulfation pattern (E) and (F) was unaltered. (A) Total amount of HS; (B) percentage of HS nonsulfated disaccharides (0S), *N*-sulfated disaccharides (*N*S), 6-*O*-sulfated disaccharides (6S), and 2-*O*-sulfated disaccharides (2S). Total sulfation is the sum of *N*-sulfate, 2-*O*-sulfate, and 6-*O*-sulfate groups in 100 disaccharides; (C) HS disaccharide composition: D0A0*:* HexAGlcNAc; D0S0: HexAGlcNS; D0A6: HexAGlcNAc(6S); D2A0: HexA(2S)GlcNAc; D0S6, HexAGlcNS(6S); D2S0: HexA(2S)GlcNS; D26S: HexA(2S) GlcNS(6S); (D) Total amount of CS; (E) Percentage of CS nonsulfated disaccharides (0S), 2-*O*-sulfated disaccharides (2S), 6-*O*-sulfated disaccharides (6S), and 4-*O*-sulfated disaccharides (4S). Total sulfation is the sum of 2-*O*-sulfate, 6-*O*-sulfate and 4-*O*-sulfate groups in 100 disaccharides; (F) CS disaccharide composition: D0a0: HexAGalNAc; D0a4: HexA-GalNAc(4S); D0a6: HexAGalNAc(6S); D0a10: HexAGalNAc(4S, 6S); D2a6 HexA(2S)GalNAc(6S). Data are mean values $\pm$ s.e.m. $n = 6$. Statistical significance was calculated by two-way ANOVA with Bonferroni post-test. $n = 6$, * $p < 0.05$, ** $p < 0.01$. Disaccharide abbreviations are according to the published structural code in Lawrence et al., (2008) [61]. (For interpretation of the references to color in this figure legend, the reader is referred to the web version of this article.)

size distribution of CS was similar to that in wild type chondrocytes. The compensation of reduced HS levels by CS seems thus not to be a unique feature of differentiated chondrocytes.

Reduced HS 2-*O*-sulfation results in increased CS levels

As chondrocytes compensate severely reduced HS levels by elevating their CS content, we next asked how cells respond to an altered HS structure. To avoid redundancy by homologous enzymes, we investigated mice deficient in *Hs2st1*, the only HS 2-*O*-sulfotransferase expressed in mammals. We first studied the abundance of HS and CS epitopes on forelimb sections of E16.5 Hs2st1 deficient mice by immunofluorescence analyses. We found reduced abundance of the 10E4 epitope, while the ΔHS epitope, recognized by the 3G10 antibody, seemed to be increased in the mutant cartilage (Fig. 5(A) and (C)). Similar to the *Ext1*$^{gt/gt}$ mice, the level of the sulfated CS neoepitopes ΔDi-4S and ΔDi-6S was increased in the mutant cartilage, while for the nonsulfated neoepitope ΔDi-0S the increase was less pronounced (Fig. 5(B) and (C)).

Analysis of the total amount of GAGs by carbazole assay revealed an increase of CS by 25% in E15.5 *Hs2st1*$^{-/-}$ skeletons compared to control littermates (Fig. 5(D)). Detailed analysis of the GAG composition by RPIP-HPLC revealed no significant difference in the HS amount of wild type and *Hs2st1*$^{-/-}$ mice (Fig. 6(A)). As expected, 2-*O*-sulfated disaccharides were only detected at background level in HS from *Hs2st1*$^{-/-}$ skeletons. The loss of di-and trisulfated disaccharides containing 2-*O*-sulfation was partially compensated by an increase of mono- and disulfated species carrying *N*-sulfate groups. Nevertheless, the total HS sulfation level was reduced compared to that of wild type chondrocytes (Fig. 6 (B) and (C)). Interestingly, similar to our observation in *Ext1*$^{gt/gt}$ chondrocytes, we found elevated amounts of CS (31%) in *Hs2st1*$^{-/-}$ chondrocytes (Fig. 6(D)), while the CS composition was not altered compared to wild type littermates (Fig. 6(E) and (F)).

To investigate whether cells respond to the altered HS sulfation pattern by modifying the size of the

Table 1. Relative distribution of ^{35}S-labeled CS and HS in mutant and control chondrocyte cultures. [^{35}S]Sulfate-labeled GAGs isolated from primary differentiated *Ext1*$^{gt/gt}$, *Hs2st*$^{-/-}$ and control chondrocytes were separated by size exclusion chromatography before and after CSase ABC or HNO_2 (pH 1.5 and 3.9) cleavage, respectively. The relative amounts of HS and CS in the polymer and dp2 peak obtained by each treatment were quantified. The values given for HS [%] are the mean of the GAG fraction insusceptible to CSase ABC digestion and the fraction degraded by treatment with HNO_2. The corresponding values for CS [%] are the mean of the fraction insusceptible to HNO_2 treatment and the fraction degraded by CSase ABC.

	Ext1 contr		*Ext1*$^{gt/gt}$		*Hs2st* contr		*Hs2st*$^{-/-}$	
	HS [%]	CS [%]	HS [%]	CS [%]	HS [%]	CS [%]	HS [%]	CS [%]
CL	47 ± 4	43 ± 8	30 ± 6	61 ± 10	45 ± 1	48 ± 3	58 ± 2	37 ± 3
CM I	9 ± 2	88 ± 2	4 ± 2	93 ± 2	9 ± 2	83 ± 8	9 ± 0.1	86 ± 4
CM II	9 ± 5	89 ± 6	4 ± 2	92 ± 2	7 ± 1	89 ± 1	8 ± 2	88 ± 2

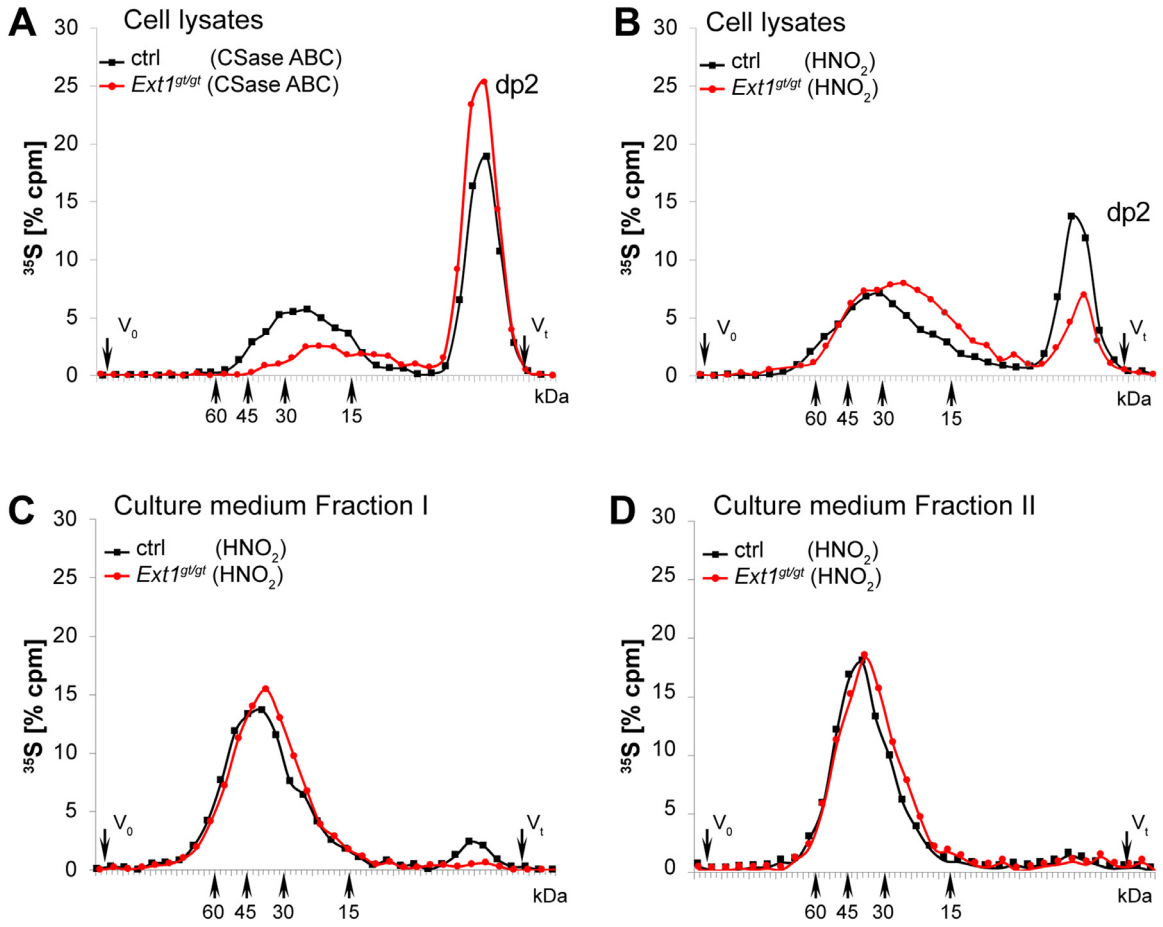

Fig. 3. Reduced CS chain length in *Ext1*$^{gt/gt}$ chondrocytes. [^{35}S]Sulfate-labeled GAGs from cell-lysates (A) and (B), and culture medium (C) and (D) isolated from intact proteoglycans (see "Experimental Procedures" and Supplementary Fig. 1) of control and *Ext1*$^{gt/gt}$ primary differentiated chondrocytes were analyzed by size exclusion chromatography on a Superose 6 column. (A) The cell-surface-associated HS chains of *Ext1*$^{gt/gt}$ cells remaining after Chondroitinase ABC digestion *(red circles)*, were of reduced size compared to the HS chains of control cells *(black squares)*. (B) More *Ext1*$^{gt/gt}$ CS chains, obtained after HNO_2 digestion, were shifted towards lower molecular weight compared to control CS chains. (C) and (D) Similarly, the CS chains of both, high molecular (Culture medium fraction I) and low molecular weight proteoglycans (Culture medium fraction II) were slightly reduced size in *Ext1*$^{gt/gt}$ cells. Data are represented as [%] of the input. V_0: void volume, V_t: total column volume, dp2: degradation products, mainly disaccharides. The sizes of saccharide standards are indicated. *n* = 3. One representative experiment is shown. (For interpretation of the references to color in this figure legend, the reader is referred to the web version of this article.)

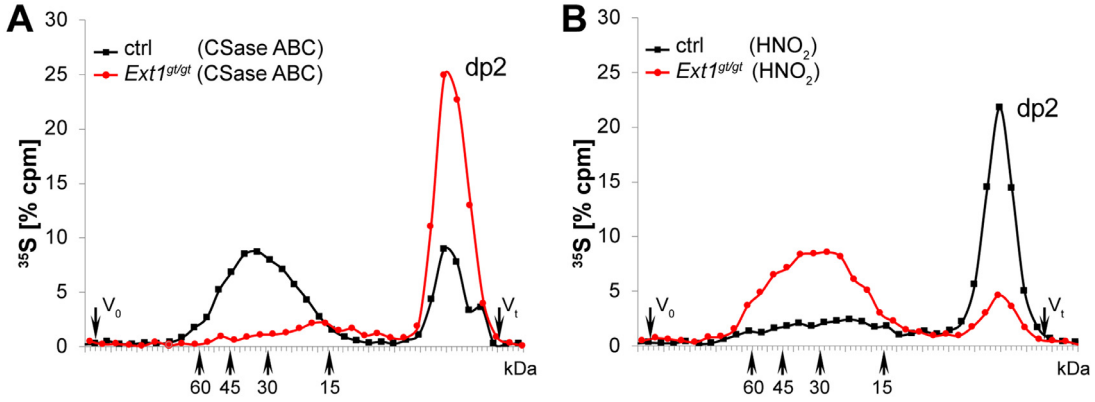

Fig. 4. CS dominates in primary limb mesenchymal cells of *Ext1*$^{gt/gt}$ embryos. [^{35}S]Sulfate-labeled GAGs purified from primary limb mesenchymal *Ext1*$^{gt/gt}$ and control cell lysate (see Fig. 3) were analyzed by Superose chromatography following digestion with Chondroitinase ABC (A) or HNO_2 (B). No alterations in GAG chain length were observed. While negligible levels of HS were synthesized in *Ext1*$^{gt/gt}$ cells (A, *red circles*), CS was the predominant GAG in these cells (B, *red circles*). $n = 2$. One representative experiment is shown. (For interpretation of the references to color in this figure legend, the reader is referred to the web version of this article.)

GAG chains, ^{35}S-labeled GAGs were isolated from differentiated chondrocytes cultured in the presence of [^{35}S]sulfate and analyzed by size exclusion chromatography (see Supplementary Fig. 1). Our analysis revealed that the length of cell-surface-associated HS chains was slightly increased in *Hs2st1*$^{-/-}$ chondrocytes, while CS chains were of similar length to those of wild type chondrocytes (Fig. 7(A) and (B), Supplementary Fig. 2(E) and (F)). This was also the case for CS chains found on PGs of the CM I fraction, while the chains of fraction CM II seemed to be slightly longer in mutant chondrocytes (Fig. 7(C) and (D)).

Together these results demonstrate that chondrocytes respond not only to reduced HS levels but also to an altered HS structure with complex compensatory mechanisms including changes in HS structure and an increased production of CS.

Mild alterations in gene expression of GAG synthesizing enzymes and core proteins

To gain insight into the mechanisms leading to the altered GAG composition, we analyzed the gene expression of key enzymes of the respective synthesis pathways and common core proteins by quantitative RT-PCR of E15.5 forelimb cartilage elements (Fig. 8). Surprisingly, the expression of most synthesizing enzymes was not significantly altered in either mouse strain. Nevertheless, more alterations were found in the *Ext1*$^{gt/gt}$ mutants (Fig. 8(A)). Together with the expected downregulation of *Ext1*, we found significantly increased expression of *Glce* and *Hs2st1*. Of the CS synthesizing enzymes, only the expression of *CSGalNAcT1*, which initiates the CS chain, was increased. In *Hs2st1*$^{-/-}$ chondrocytes, only the mRNA level of *Ext2* was decreased besides the expected downregulation of *Hs2st1* (Fig. 8(C)).

Analysis of the HS-carrying core proteins revealed an increased expression of the GPI-anchored glypicans (Gpc), *Gpc2, Gpc3* and *Gpc6* in *Ext1*$^{gt/gt}$ chondrocytes (Fig. 8(B)). In addition, *agrin (Agrn)*, which encodes a PG secreted into the ECM was increased. Of the CS/DS carrying core proteins, the small leucin-rich proteoglycan *decorin (Dcn)* was reduced, while the expression of *biglycan (Bgn)* was elevated. Importantly, the expression of *aggrecan (Acan)* the major PG of the interterritorial ECM, was increased, accompanied by an increased expression of the *hyaluronan binding link protein* (*Hpln1*). In the *Hs2st1* mutants, *Dcn* was the only CSPG core protein showing significantly reduced expression, while the expression levels of *Acan* and *Hapln1* were slightly increased (Fig. 8(D)).

CS dependent alterations in BMP and FGF signaling

To investigate the role of CS as a regulator of growth factor signaling in chondrocytes, we investigated the phosphorylation of Erk (pErk) and Smad1/5/9 (pSmad1/5/9) as a readout for Fgf18 and Bmp2 signaling before and after removal of CS by chondroitinase ABC treatment. Surprisingly, loss of CS resulted in an immediate increase in pErk levels even without Fgf18 treatment (Fig. 8 (E)). To test if this is a specific response of chondrocytes we analyzed pErk levels in LMCs and found a similar upregulation upon CS removal (Supplementary figure 3A) pointing to an important role of CS in regulating or storing signaling molecules. Treatment of differentiated chondrocytes with BMP2 resulted in an increased phosphorylation of Smad1/5/9, which was reduced after CSase treatment in wild type, *Ext1*$^{gt/gt}$ and *Hs2st1*$^{-/-}$

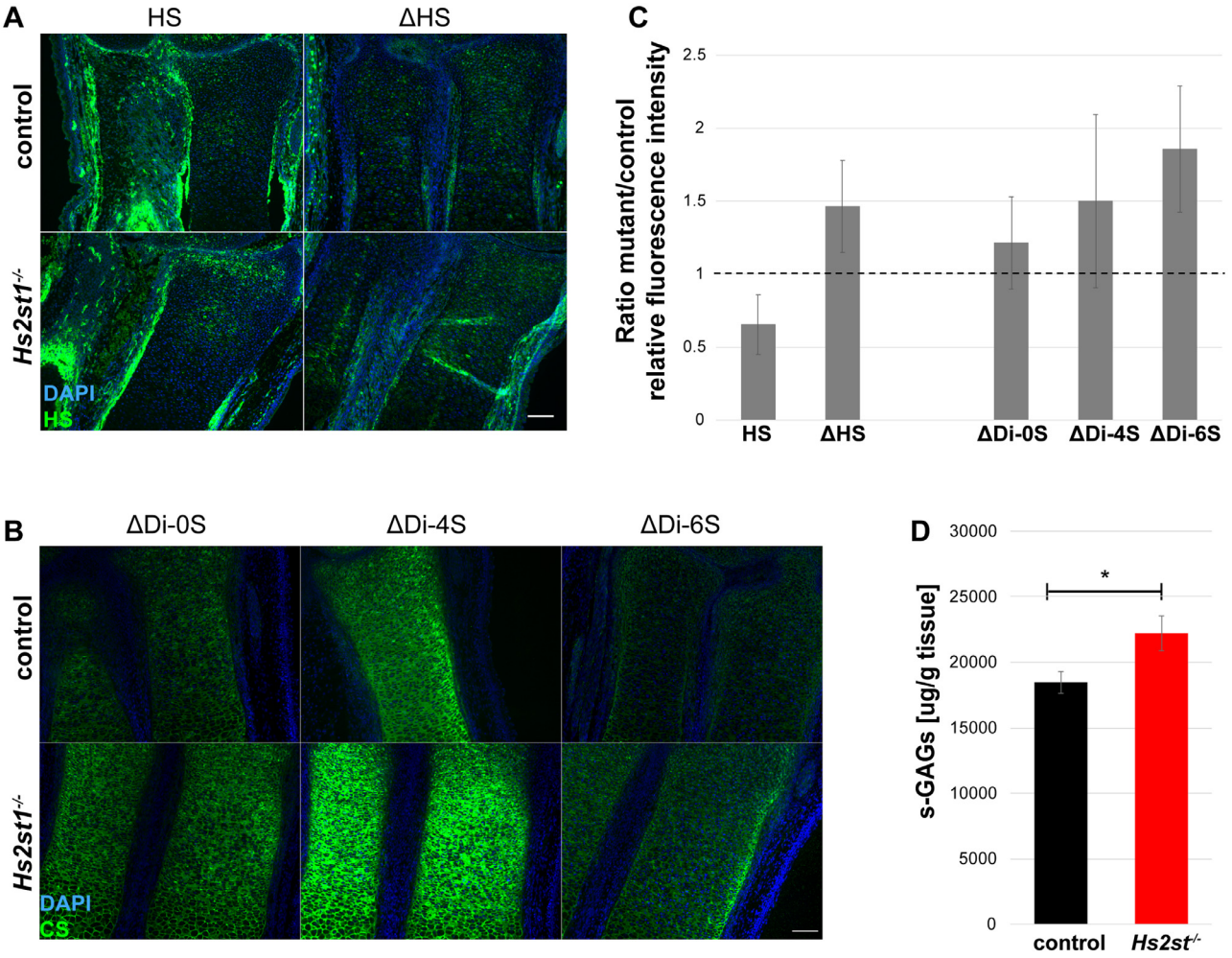

Fig. 5. Loss of 2-*O*-sulfation leads to increased CS levels. Forelimb sections of E15.5 *Hs2st*$^{-/-}$ and control embryos were probed with monoclonal antibodies (*green*) recognizing native chains (HS), the HS neoepitope (ΔHS) (A), and the CS neoepitopes ΔDi-0S, ΔDi-4S, ΔDi-6S (B). Sections were counterstained with DAPI (*blue*). (A, B) In *Hs2st*$^{-/-}$ forelimb cartilage, the HS and the sulfated CS neoepitopes were increased, while total HS (HS) and the CS neoepitope ΔDi-0S were not considerably altered. (C) Analysis and quantification of fluorescence images were performed as in Fig. 1. $n = 3$. (D) Quantification of sulfated GAGs purified from E15.5 *Hs2st*$^{-/-}$ and control skeletal element using the carbazole assay showed an increase in the GAG amount of 25% in *Hs2st*$^{-/-}$ mutants. Values are normalized to tissue dry weight and shown as mean ± *s*.e.m. $n = 4$. Statistical significance was calculated by unpaired, two-tailed Student's *t*-test. * $p < 0.05$. Scale bars: 100 μm (A) and (B). (For interpretation of the references to color in this figure legend, the reader is referred to the web version of this article.)

chondrocytes, (Fig. 8(F) and Supplementary Fig. 3 (B)). CS seems thus to support Bmp signaling.

Discussion

In this study, we have characterized the composition of HS and CS in two mouse strains with an altered HS biosynthesis: *Ext*$^{gt/gt}$ mice, which synthesize low levels of HS, and *Hs2st1*$^{-/-}$ mutants in which the pattern of HS sulfation is disturbed. We found that not only a reduced HS level but also an altered HS structure results in an increased production of CS. To our knowledge, this is the first in vivo study demonstrating that a mammalian tissue compensates an altered HS structure with increased CS levels and distinct alterations in CS and HS chain length.

Alterations in HS structure lead to increased CS levels

Detailed analysis of the GAG composition revealed that *Ext*$^{gt/gt}$ chondrocytes produce about 20% HS, while the HS level in *Hs2st1* mutants is unchanged. Interestingly, both mutants respond to the altered HS production by distinct changes in the HS sulfation pattern, which has also been observed in other mice with an altered HS structure [42-46]. The HS of *Ext1*$^{gt/gt}$ mutants contains more di- and

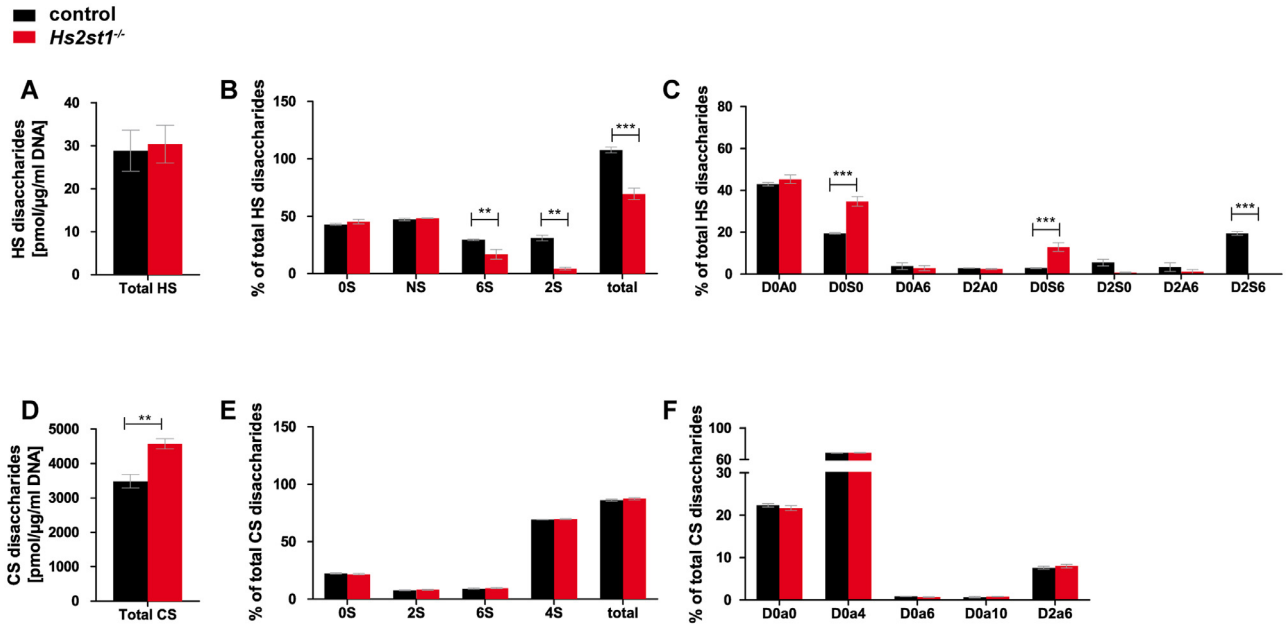

Fig. 6. Hs2st deficiency leads to alterations in the HS but not in the CS structure. The amount and disaccharide composition of HS and CS isolated from E15.5 *Hs2st*$^{-/-}$ (*red*) and control (*black*) skeletal elements were analyzed by RPIP-HPLC. (A) and (D) The total amount of HS was not altered in *Hs2st1*$^{-/-}$ mutants, while the CS level was increased by 31%. (B) and (C) HS 2-*O*- and 6-*O*-sulfation as well as total sulfation were decreased in *Hs2st1*$^{-/-}$ chondrocytes, due to loss of D2S6 disaccharides and despite an increase in D0S0 and D0S6 disaccharides. (E) and (F) The CS sulfation pattern was unaltered. (A) Total amount of HS; (B) Percentage of HS nonsulfated disaccharides (0S), *N*-sulfated disaccharides (*N*S), 6-*O*-sulfated disaccharides (6S), and 2-*O*-sulfated disaccharides (2S). Total sulfation is the sum of *N*-sulfate, 2-*O*-sulfate, and 6-*O*-sulfate groups in 100 disaccharides; (C) HS disaccharide composition, see legend to Fig. 3 for explanation of abbreviations; (D) Total amount of CS; (E) Percentage of CS nonsulfated disaccharides (0S), 2-*O*-sulfated disaccharides (2S), 6-*O*-sulfated disaccharides (6S), and 4-*O*-sulfated disaccharides (4S). Total sulfation is the sum of 2-*O*-sulfate, 6-*O*-sulfate and 4-*O*-sulfate groups in 100 disaccharides; (F) CS disaccharide composition, see legend to Fig. 3 for explanation of abbreviations. Data are mean values ± s.e.m. $n = 6$. Statistical significance was calculated by two-way ANOVA with Bonferroni post-test. $n = 6$, * $p < 0.05$, ** $p < 0.01$. (For interpretation of the references to colour in this figure legend, the reader is referred to the web version of this article.)

trisulfated disaccharides resulting in higher relative amounts of 6-*O*-sulfation. In contrast, Yamada et al. did not find changes in HS sulfation of *Ext1*$^{gt/gt}$ embryonic fibroblasts [35]. Similar to *Ext1*$^{gt/gt}$ mutant HS, HS of *Hs2st1*$^{-/-}$ chondrocytes contains elevated levels of mono *N*-sulfated disaccharides and disulfated disaccharides carrying *N*- and 6-*O*-sulfate groups. Nevertheless, due to the loss of 2-*O*-sulfated disaccharides the *Hs2st1*$^{-/-}$ chondrocytes do not manage to reach the total sulfation degree of control cells. Different to our findings, *Hs2st1*$^{-/-}$ embryonic fibroblasts maintain the overall charge density of the mutant HS by increasing both, *N*- and 6-*O*-sulfation, mostly present in disulfated disaccharides [46]. Apparently, the HS biosynthesis machinery responds differently to an altered HS production in embryonic fibroblasts and chondrocytes.

Interestingly, while the sulfation pattern of HS is changed beyond the genetically induced deficiency in both mutant strains, we did not identify differences in the sulfation pattern of CS. Instead, we observed a substantial increase in the amount of CS in *Ext*$^{gt/gt}$ mutants and, even more surprisingly, in *Hs2st1*$^{-/-}$ chondrocytes. A compensation of HS by CS has been described before in HS-deficient CHO and embryonic stem cells [6,32,47]. In *Ext1*$^{-/-}$ embryonic stem cells and embryoid bodies, the elevated CS amount was approximately equivalent to the loss of HS, leading to the hypothesis that the pool of unused precursors, like uridine diphosphate sugars and the sulfate donor 3′phosphoadenosine-5′phosphosulfate (PAPS), drives the increased CS synthesis [32]. The interdependence of HS and CS synthesis has also been investigated in different zebrafish mutants [48]. In this study, loss of *Extl3,* and thereby loss of HS-chain initiation, leads to increased CS synthesis, while a morpholino-induced inactivation of CSGalNAcT1/2 slightly increased HS amounts. In contrast to our results, a substantial reduction of HS levels, in this case, due to loss of Ext2, did not increase CS levels. This led to the hypothesis that the balance between the chain-initiating enzymes is the critical factor determining the relative levels of HS and CS. However, our results clearly demonstrate that not only a chain-initiation-independent reduction of HS synthesis but also an

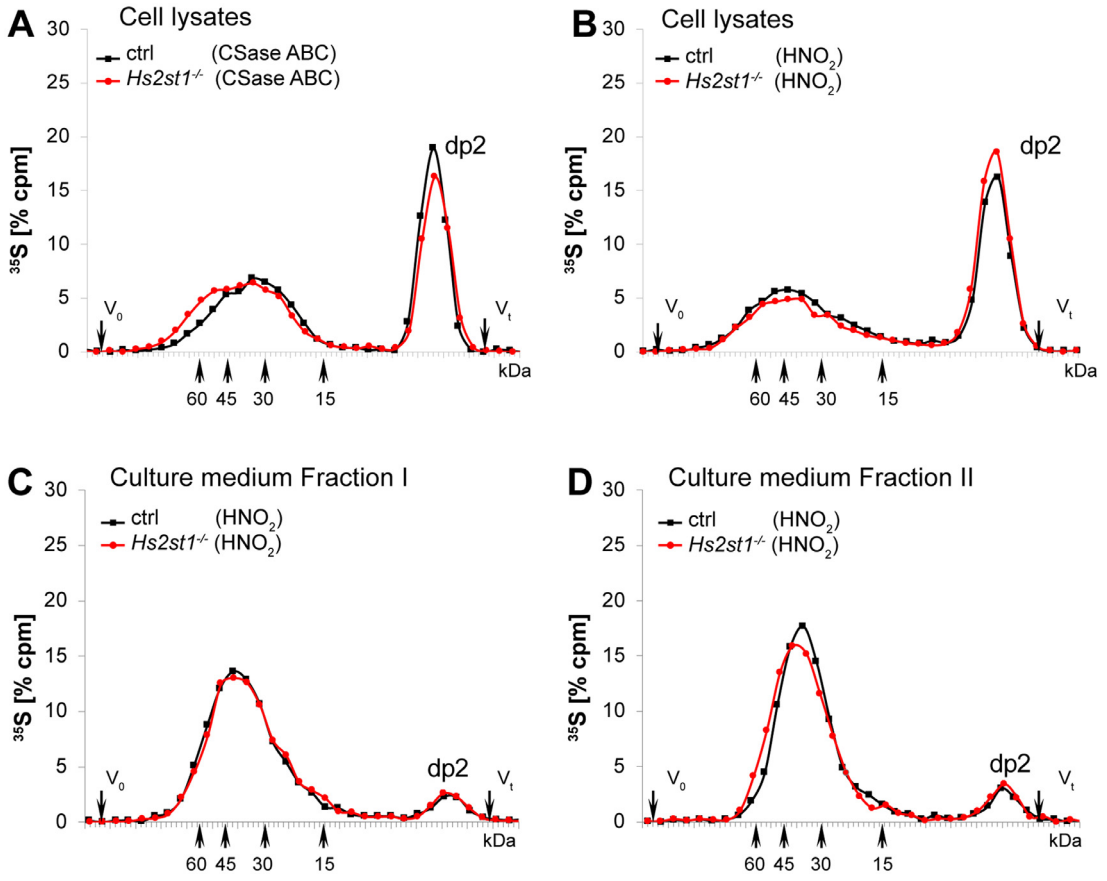

Fig. 7. Altered size distribution of GAGs synthesized by Hs2st$^{-/-}$ chondrocytes. [^{35}S]Sulfate-labeled GAGs from cell lysates (A) and (B) and culture medium (C) and (D) isolated from intact proteoglycans (see "Experimental Procedures" and Supplementary Fig. 1) of control and *Hs2st1*$^{-/-}$ primary differentiated chondrocytes were analyzed by size exclusion chromatography on a Superose 6 column. (A) While the HS chains of the *Hs2st1*$^{-/-}$ cells remaining after CSase ABC digestion (*red circles*) were longer compared to the control cells (*black squares*), (B) no alteration in CS chain length was observed. (C) The length of the secreted CS chains of fraction CM I was not altered, while the CS chains of fraction CM II (D) were slightly longer. Data are represented as [%] of the input. V_0: void volume, V_t: total column volume, dp2: degradation products, mainly disaccharides. The sizes of saccharide standards are indicated. (A), (B) $n = 5$; (C), (D) $n = 3$. One representative experiment is shown. (For interpretation of the references to color in this figure legend, the reader is referred to the web version of this article.)

altered HS structure leads to increased CS levels. Furthermore, the stoichiometry of HS and CS in chondrocytes strongly supports a yet unidentified, precursor-independent mechanism, which senses the amount and quality of HS in an environment that contains a vast excess of CS. Whether such a sensing mechanism is directly linked to the synthesis machinery in the Golgi apparatus or involves specific yet unknown extracellular receptors has to be investigated in future studies. In this respect, it is interesting to note that loss of *Ext1* in embryonic stem cells [32] or chondrocytes [49] leads to a cell-autonomous upregulation of Smad2 and Smad1/5/8 phosphorylation, respectively. One might thus speculate that altered growth factor signaling contributes to the changes in the GAG composition.

Another unsolved question addresses the mechanism by which CS levels are increased. Interestingly, the expression of most HS or CS synthesizing enzymes is not dramatically changed in either mutant strongly pointing to a regulation on protein level.

Chondrocytes produce more, instead of longer CS chains

To understand if altered CS levels are due to an increase in length or chain number, we investigated the size and distribution of HS and CS chains in primary differentiated chondrocytes. We found that the vast majority of the ^{35}S-labeled GAGs is secreted into the ECM and consists almost exclusively of CS, while similar amounts of HS and CS are present on the cell surface. This distribution reflects the localization of PGs in chondrocytes, in which the majority of HSPGs like syndecans or glypicans are associated

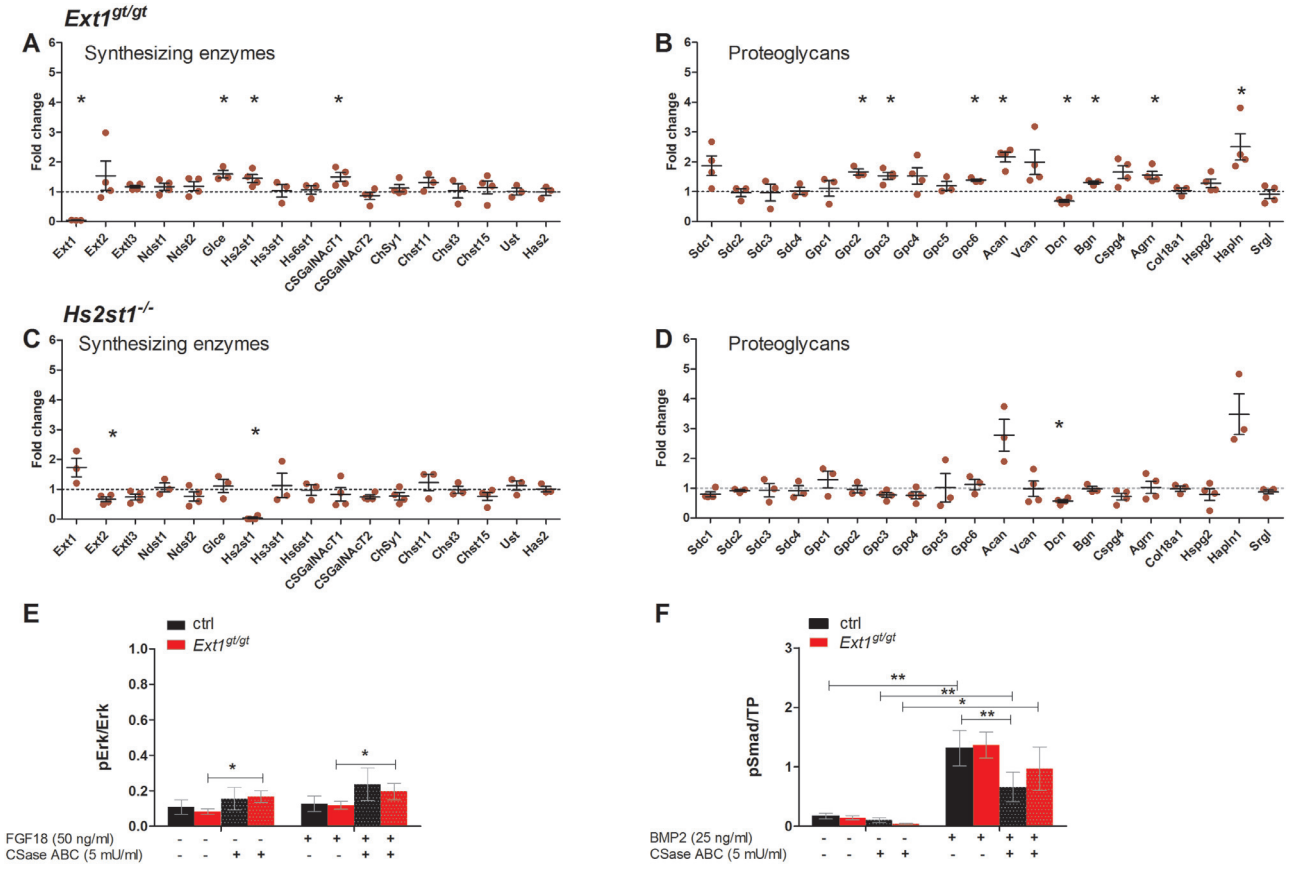

Fig. 8. An altered HS structure leads to distinct alterations in PG synthesis and growth factor signaling. The expression level of GAG biosynthesis enzymes (A) and (C) and selected PG core proteins (B) and (D) in cartilage elements of E15.5 *Ext1*$^{gt/gt}$ (A) and (B), *Hs2st*$^{-/-}$ (C) and (D) and control littermates were evaluated by quantitative RT-PCR. Data are represented as fold change (ΔΔ-CT value) relative to β2M expression and control littermates. *n* = 3. Fgf18 (pErk/Erk, (E)) and Bmp2 (pSmad1/5/9/TP (F)) signaling was analyzed in primary *Ext1*$^{gt/gt}$ and wild type differentiated chondrocytes with or without chondroitinase ABC treatment. (A) Control and *Ext1*$^{gt/gt}$ mice responded to a similar degree to Bmp2 treatment. The response was diminished when chondroitin sulfate was digested prior to the Bmp2 stimulation. (E) CS removal leads to increased pErk levels independent of FGF18 treatment and to a reduced response to Bmp2 treatment (F). Values are shown as mean ± s.e.m. Statistical significance was calculated by two-way ANOVA with Bonferroni post-test. Measurements were performed in technical duplicates. n indicates biological replicates. (A) *n* = 3, (B) *n* = 5

with the cell surface, while aggrecan, the most abundant cartilage PG, which may carry up to 100 CS chains, is located in the interterritorial ECM.

As has been observed in MEFs [35], loss of *Ext1* in chondrocytes also leads to a decreased HS chain length. CS chains of the cellular fraction show a broad size distribution in both, mutant and wild type cells, but a larger fraction of the CS chains from the *Ext1*$^{gt/gt}$ cells distributes towards smaller molecular size. A small but reproducible decrease in chain length was also seen for the CS chains of the secreted PGs. In *Hs2st1* mutants, the length of the HS chains was increased, while no alteration in CS chain length was observed, except for a slight increase in the secreted fraction CMII. Together with the increased level of CS neoepitopes detected by the immunofluorescence analysis, these results strongly indicate that the increase in CS levels is mainly due to the production of additional chains and not to the synthesis of longer chains.

This leads to the question, to which core proteins the additional CS is bound. In the *Ext1* mutants, the secreted PG biglycan, which carries two CS/DS chains is upregulated, while the one side chain carrying decorin is expressed at lower levels. While biglycan might contribute to the increased amounts of CS , its expression level hardly explains the massive increase of CS in the mutants. In contrast, in both mutants, *Acan* expression is upregulated making it likely that the majority of the additional CS chains are attached to the aggrecan core protein. The vast increase in chain-initiation points might then deplete the CS precursor pool resulting in a shortening of the chains.

While aggrecan might carry most of the secreted CS, the association of CS to specific PGs on the cell

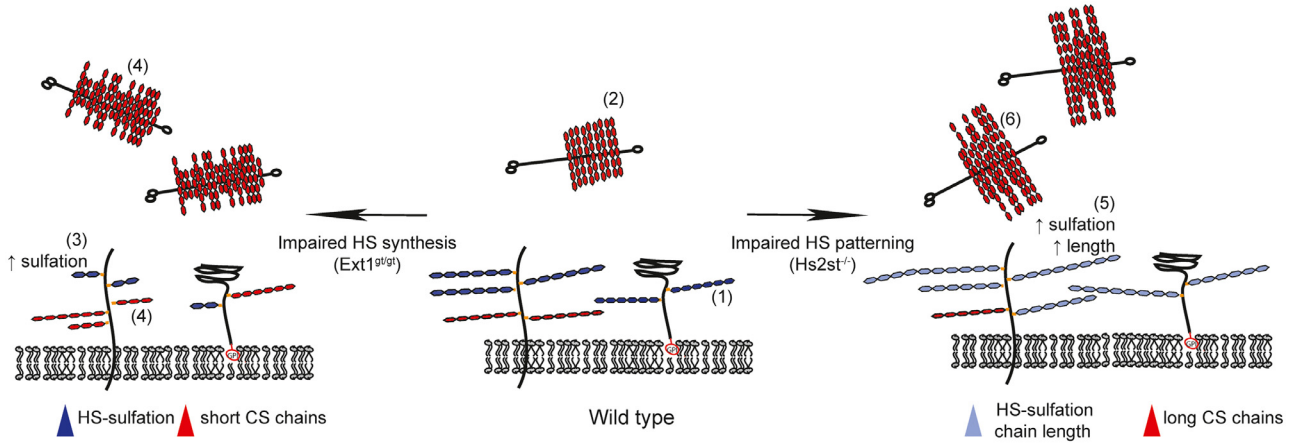

Fig. 9. An altered HS structure is compensated by increased CS levels in chondrocytes. In wild type chondrocytes (*center*), PGs carrying HS (*blue*, (1)) and CS (*red*, (2)) chains decorate the plasma membrane or are secreted into the interterritorial matrix. Reduced levels of HS (*left panel*) in *Ext1*$^{gt/gt}$ chondrocytes trigger a compensatory mechanism resulting in increased sulfation of the remaining HS chains (3). Additionally, chondrocytes double the amount of CS by producing more but shorter chains (4). *Hs2st1*$^{-/-}$ chondrocytes (*right panel*) increase the level of sulfated disaccharides (*light blue*) not affected by the mutation and elongate the HS chains (5). In addition, they increase the amount and size of the secreted CS (6). In both mutants, the additional CS is mainly secreted and bound to aggrecan. (For interpretation of the references to color in this figure legend, the reader is referred to the web version of this article.)

surface is more difficult to explain. No CS-carrying PG is obviously upregulated, leading to the hypothesis that attachment sites less frequently used for CS substitution or such normally occupied by HS harbor CS chains in the mutants. It has previously been shown that modification of the tetrasaccharide linkage region affects the type of GAG chains synthesized [50,51], providing a potential mechanism to increase the CS attachment points. In accordance with this hypothesis, Holmborn et al. observed a higher number of CS-substitutions on zebrafish syndecan-4 after siRNA-dependent silencing of Extl3 [48]. We did, however, not detect any decrease in HS neoepitopes in either analyzed mutant, making it unlikely that the increased CS levels depend on CS polymerization on sites normally carrying HS.

As shown in Fig. 4 and demonstrated before [32,52], not only chondrocytes but also primary limb mesenchymal cells and ES cells, increase their CS content as a response to reduced HS levels leading to the question whether all tissues react in a similar way. If so, why does the altered HS structure lead to generally less severe phenotypes in chondrocytes compared to other cell types? One reason might be the unusually high level of CS in chondrocytes, which might contribute to the regulation of signaling factors under normal conditions. First analyses of Fgf18 and Bmp2 signaling, two important regulators of chondrocyte differentiation, revealed a CS-dependent activity strongly pointing to a function of CS as a regulator of growth factor signaling in chondrocytes. If this function is mainly due to the storage of growth factors, as indicated by the Fgf18-independent upregulation of pERK, or by a direct regulation of signaling, as suggested by the reduced pSmad1/5/8 levels, will require detailed further studies. Nevertheless, the obtained data point to a yet underestimated importance of the HS/CS composition in regulating tissue homeostasis.

Conclusions

In summary, our experiments give new and important insight into the regulation of sulfated GAG biosynthesis in chondrocytes. We demonstrate that increased amounts of CS are produced to compensate for alterations of the HS composition (Fig. 9). Although other studies have found increased CS synthesis as a response to reduced HS levels, an altered sulfation pattern has not been shown before to affect the synthesis of CS. In addition, our results together with the data obtained by Holmborn et al., [48], strongly support the hypothesis that cells try to maintain a certain level of HS sulfation on the cell surface by compensating an altered HS composition with increased sulfation at mutation-independent positions. Likewise, the elongated chain length observed in *Hs2st1*$^{-/-}$ mutants might be an additional attempt to restore the abnormal HS, which is hampered in *Ext1*$^{gt/gt}$ chondrocytes. If, however, HS sulfation cannot sufficiently be increased, cells increase their CS content (Fig. 9). This is in accordance with the role of HS as a regulator of many signaling pathways, which require the interaction of HS for ligand-receptor binding or the control of ligand distribution. As CS also binds to many HS-dependent growth factors, the vast increase in CS might compensate for at least some of the lacking HS function. Our investigations of Bmp and Fgf

signaling in mutant cells strongly indicate that the interaction and relative importance of HS and CS is more complicated than previously thought and will require an in-depth analysis of the response of individual signaling pathways.

Experimental procedures

Ethics statement

Mice were kept and bred according to the institutional guidelines of the University of Duisburg-Essen and the University Hospital Essen, specifically approved by the animal welfare officer of the University of Duisburg-Essen. Mouse husbandry was approved by the city of Essen (Az: 32-2-11-80-71/348) in accordance with § 11 (1) 1a of the "Tierschutzgesetz". Work with transgenic animals was approved by the "Bezirksregierung Duesseldorf" (Az: 53.02.01-D-1.55/12, Anlagen-Nr. 1464) in accordance with § 8 Abs. 4 Satz 2 GenTG of the "Gentechnikgesetz".

Transgenic mice

For timed pregnancies, noon of the day of a vaginal plug was considered to be embryonic day (E) 0.5. Heterozygous *Ext1^{gt}* (Ext1$^{Gt(pGT2TMpfs)064Wcs}$) [12] mice were maintained on a C57Bl/6 J background. Hs2st^{f} (Hs2st1$^{tm1.1Je}$) [53] mice were crossbred to Prx1-Cre (Tg(Prrx1-Cre)1Cjt) females [54] to induce germline recombination. Hs2st1^{-} mice were maintained on a C57Bl/6J background. Genotyping was performed by genomic PCR of tail biopsies using the established primers [13] [53].

Immunofluorescence analysis and imaging

Embryonic limbs (E15.5 for *Ext1^{gt}* and E16.5 for *Hs2st1^{-}*, and wild type littermates) were prepared in phosphate-buffered saline (PBS), fixed overnight in 4% paraformaldehyde, dehydrated and embedded in paraffin. Serial sections of 6 μm thickness were then rehydrated and stained. HS epitopes were detected with mAb 10E4 and 3G10 [36] (Amsbio) following digestion with 1000 U Hyaluronidase I (Sigma-Aldrich) or 200 mU heparitinase I (Amsbio), respectively. The CS neoepitopes ΔDi-0S, ΔDi-4S and ΔDi-6S were detected with mAb 1B5, 2B6 and 3B3, respectively [38] after digestion with 50 mU Chondroitinase ABC (Sigma-Aldrich). The primary antibodies were then detected using Alexa-Fluor 488 conjugate (Thermo Fischer Scientific). The sections were counterstained with DAPI (Sigma-Aldrich). Pictures were taken on AxioObserver 7 with Axiocam 506 mono CCD camera using software Zen 2.3 (Zeiss) and Axioplan2, Axiovert 200 M (Zeiss), using MetaMorph® imaging software 6.3r6 (Molecular devices).

Image analysis

The DAPI and GFP fluorescence intensity were measured in identical region of columnar proliferating chondrocytes (Fig. 1(A), white rectangle), taken in the respective channel using Fiji (1.52e) Software [55]. The Corrected total cell fluorescence (CTCF) was calculated as described before [56]. CTCF value of the desired probe was normalized to CTCF of the nuclear DAPI staining. Data are shown as mean values ± s.e.m., relative to the control set to 1.

Real-time quantitative PCR analysis

E15.5 forelimbs were manually freed from the surrounding tissues in PBS under a stereomicroscope. RNA was purified using NucleoSpin® RNA Plus RNA isolation kit (Macherey-Nagel). cDNA was synthesized using Maxima first strand cDNA synthesis (Thermo Fischer Scientific) according to the manufacturer's instructions. RT-qPCR measurements were carried out on a CFX384 Touch™ Real-Time PCR detection system using EVA green PCR master mix (Bio-Budget Technologies GmbH). Amplification efficiencies were determined using serial dilutions of the template. Primer specificity was confirmed analyzing the melting-curves. Relative gene expression was calculated by the $2^{-\Delta\Delta Ct}$ method [57] and was normalized to the reference gene β2-microglobulin (*β2m*) and a littermate control sample. Primers used to detect targeted genes are listed in SupplementaryTable 1. Primer for *Gpc2* and *Agrn* were described before [20,58].

Primary chondrocyte culture

Fore- and hindlimbs of E13.5 mouse embryos were dissected in sterile PBS (Gibco) and sequentially digested with Neutral Protease (1 U/ml, Serva) and digestion cocktail containing Collagenase NB4 (0.3 U/ml; Serva), 5% fetal calf serum (FCS, PanBiotech) and 0.05% Trypsin-EDTA (Invitrogen). Cells were passed through a 40 μm Falcon cell strainer (DB) and cultured in DMEM/F-12 (Gibco) supplemented with 10% FCS and 1% penicillin/streptomycin (Invitrogen). Primary cells were either expanded for 24 h (analysis of undifferentiated limb mesenchymal cell) or allowed to reach 100% confluency and differentiated in DMEM/F-12 medium supplemented with 5% FCS and 1% Insulin-Transferrin-Selenium (ITS) (Life Technologies) for five days.

Analysis of FGF and BMP signaling

1×10^5 primary Ext1$^{gt/gt}$, Hs2st$^{-/-}$ and control chondrocytes were seeded in 24-well plates and

cultured as described above. Cell were washed in PBS and starved in serum free DMEM/F-12 medium supplemented with 1% ITS 24 h prior to analysis. Cells were treated with or without Chondroitinase ABC (5 mU/ml) for 30 min at 37 °C followed by stimulation with FGF18 (25 or 50 ng/ml) or BMP2 (25 ng/ml) for 15 min at 37 °C. Immunoblot analysis of cell lysates was performed using monoclonal mouse anti-α-p44/42 MAPK (Erk1/2), rabbit anti- αphospho-Smad1/5/9 (Cell Signaling Technology) rabbit αphospho-p44/42 MAPK (pErk1/2) (Santa Cruz Biotechnology) and fluorochrome labeled secondary antibodies (Li-COR Bioscience). Total protein amount was measured using the Revert total protein stain (Li-COR Bioscience). Signal intensity was quantified using the Odyssey CLx and Image Studio software (LI-COR), and quantified against total protein (pSmad 1/5/9) or p44/42 MAPK signal (pErk).

Isolation and characterization of ^{35}S-labeled GAGs

Primary cells were incubated with 100 μCi/ml [^{35}S] sulfate supplemented in the cell culture medium for 16 h before harvest. The [^{35}S]sulfate-labeled PGs were purified from cell lysates and culture media by DEAE ion-exchange chromatography (GE Healthcare) followed by a preparative separation on a Superose 6 column 10/300 (GE Healthcare) (Supplementary Fig. 1) [41]. The ^{35}S-labeled GAG chains were released from the core proteins by alkali treatment (0.5 M NaOH overnight at 4 °C followed by neutralization with HCl). The ^{35}S-labeled GAG, HS and CS chains were then subjected to size exclusion chromatography on a Superose 6 column 10/300 (GE Healthcare) before and after treatment with Chondroitinase ABC (1 mU, Amsbio) and combined nitrous acid deamination at pH 1.5 and pH 3.9 [59], respectively. Samples were eluted with 1 M NaCl, 50 mM Tris−HCl, pH 7.5, 0.1% Triton X-100. Fractions of 0.5 ml were collected and analyzed by scintillation counting.

GAG quantification and analysis

The skeletons of E15.5 *Ext1*$^{gt/gt}$ and *Hs2st*$^{-/-}$ embryos were manually freed from inner organs and surrounding tissue under a stereomicroscope as described before [20]. The HS and CS disaccharides, generated following exhaustive enzymatic depolymerization, were analyzed using reverse-phase ion-pairing (RPIP)-HPLC as described before [60]. A cocktail of heparin lyases I, II and III was used to cleave HS (IBEX Pharmaceuticals), while Chondroitinase ABC (Amsbio) was applied for CS degradation. Signals were quantified against known standards (Calbiochem). For GAG quantification using the carbazole assay, GAGs were purified as described [41] but increasing the NaCl concentration to 0.3 M. Carbazole assay was performed as described before [39,40]. The absorbance was measured in technical duplicates at 530 nm. The GAG concentration was determined using a standard curve of predefined heparin solution and normalized to tissue dry weight. Data are shown as mean values ± s.e.m.

Image analysis

The DAPI and GFP fluorescence intensity were measured in identical region of columnar proliferating chondrocytes (Fig. 1(A)), taken in the respective channel using Fiji (1.52e) Software [55]. The regions were selected using ROI Manager. The Corrected total cell fluorescence (CTCF) was calculated as described before [56]. CTCF value of the desired probe was normalized to CTCF of the nuclear DAPI staining. Data are shown as mean values ± s.e.m., relative to the control set to 1.

Statistical analyses

Statistical analyses were performed using unpaired, two-tailed Student's *t*-test and two-way ANOVA with Bonferroni post-test using GraphPad Prism version 5.0b for Mac OS X (GraphPad Software, San Diego California USA, (www.graphpad.com). Significance was assumed if $p<0.05$. n refers to biological replicates.

Declaration Competing of Interest

The authors declare no conflict of interest.

CRediT authorship contribution statement

Velina Bachvarova: Conceptualization, Formal analysis, Investigation, Methodology, Project administration, Validation, Visualization, Writing - original draft, Writing - review & editing. **Tabea Dierker:** Formal analysis, Investigation, Validation, Writing - review & editing. **Jeffrey Esko:** Writing - review & editing. **Daniel Hoffmann:** Formal analysis. **Lena Kjellen:** Conceptualization, Funding acquisition, Methodology, Project administration, Supervision, Validation, Writing - review & editing. **Andrea Vortkamp:** Conceptualization, Funding acquisition, Methodology, Project administration, Supervision, Validation, Writing - original draft, Writing - review & editing.

Acknowledgments

We would like to thank Prof. Bruce Caterson (Cardiff University) for providing the CS-neoepitope antibodies.

Funding

The project was funded by a DFG grant (Vo620/14-1) to A.V, and grants of the Swedish Cancer Society and the "Stiftelsen för proteoglykanforskning" of the Uppsala University to L.K.

The funding sources had no role in study design, data collection and analysis, decision to publish or preparation of the manuscript.

Supplementary materials

Supplementary material associated with this article can be found in the online version at doi:10.1016/j.matbio.2020.03.006.

Received 26 August 2019;
Received in revised form 11 March 2020;
Accepted 12 March 2020
Available online 20 March 2020

Keywords:
Heparan sulfate;
Chondroitin sulfate;
Ext1;
Hs2st1;
Chondrocytes;
Extracellular matrix;
Endochondral ossification

Abbreviations: HS, heparan sulfate; CS, chondroitin sulfate; Ext1, exostosin-1; Hs2st1, heparan sulfate 2-O-sulfotransferase 1; RPIP-HPLC, reverse-phase ion-pairing HPLC

References

[1] L. Kjellen, U. Lindahl, Specificity of glycosaminoglycan-protein interactions, Curr. Opin. Struct. Biol. 50 (2018) 101–108.
[2] S. Sarrazin, W.C. Lamanna, J.D. Esko, Heparan sulfate proteoglycans, Cold Spring Harb. Perspect. Biol. 3 (7) (2011).
[3] J.R. Bishop, M. Schuksz, J.D. Esko, Heparan sulphate proteoglycans fine-tune mammalian physiology, Nature 446 (7139) (2007) 1030–1037.
[4] P. Gordts, J.D. Esko, The heparan sulfate proteoglycan grip on hyperlipidemia and atherosclerosis, Matrix Biol. 71–72 (2018) 262–282.
[5] D. Stickens, B.M. Zak, N. Rougier, J.D. Esko, Z. Werb, Mice deficient in EXT2 lack heparan sulfate and develop exostoses, Development 132 (22) (2005) 5055–5068.
[6] X. Lin, G. Wei, Z. Shi, L. Dryer, J.D. Esko, D.E. Wells, M.M. Matzuk, Disruption of gastrulation and heparan sulfate biosynthesis in EXT1-deficient mice, Dev. Biol. 224 (2) (2000) 299–311.
[7] J.D. Esko, S.B. Selleck, Order out of chaos: assembly of ligand binding sites in heparan sulfate, Annu. Rev. Biochem. 71 (2002) 435–471.
[8] K. Jochmann, V. Bachvarova, A. Vortkamp, Reprint of: heparan sulfate as a regulator of endochondral ossification and osteochondroma development, Matrix Biol. 35 (2014) 239–247.
[9] M. Wuelling, A. Vortkamp, Chondrocyte proliferation and differentiation, Endocr. Dev. 21 (2011) 1–11.
[10] E. Kozhemyakina, A.B. Lassar, E. Zelzer, A pathway to bone: signaling molecules and transcription factors involved in chondrocyte development and maturation, Development 142 (5) (2015) 817–831.
[11] M. Pacifici, The pathogenic roles of heparan sulfate deficiency in hereditary multiple exostoses, Matrix Biol. 71–72 (2018) 28–39.
[12] K.J. Mitchell, K.I. Pinson, O.G. Kelly, J. Brennan, J. Zupicich, P. Scherz, P.A. Leighton, L.V. Goodrich, X. Lu, B.J. Avery, P. Tate, K. Dill, E. Pangilinan, P. Wakenight, M. Tessier-Lavigne, W.C. Skarnes, Functional analysis of secreted and transmembrane proteins critical to mouse development, Nat. Genet. 28 (3) (2001) 241–249.
[13] L. Koziel, M. Kunath, O.G. Kelly, A. Vortkamp, Ext1-dependent heparan sulfate regulates the range of ihh signaling during endochondral ossification, Dev. Cell 6 (6) (2004) 801–813.
[14] Y. Matsumoto, K. Matsumoto, F. Irie, J. Fukushi, W.B. Stallcup, Y. Yamaguchi, Conditional ablation of the heparan sulfate-synthesizing enzyme Ext1 leads to dysregulation of bone morphogenic protein signaling and severe skeletal defects, J. Biol. Chem. 285 (25) (2010) 19227–19234.
[15] J.P. Li, F. Gong, A. Hagner-McWhirter, E. Forsberg, M. Abrink, R. Kisilevsky, X. Zhang, U. Lindahl, Targeted disruption of a murine glucuronyl C5-epimerase gene results in heparan sulfate lacking L-iduronic acid and in neonatal lethality, J. Biol. Chem. 278 (31) (2003) 28363–28366.
[16] V.A. Wilson, J.T. Gallagher, C.L. Merry, Heparan sulfate 2-O-sulfotransferase (Hs2st) and mouse development, Glycoconj J. 19 (4–5) (2002) 347–354.
[17] S.L. Bullock, J.M. Fletcher, R.S. Beddington, V.A. Wilson, Renal agenesis in mice homozygous for a gene trap mutation in the gene encoding heparan sulfate 2-sulfotransferase, Genes Dev. 12 (12) (1998) 1894–1906.
[18] K. Grobe, M. Inatani, S.R. Pallerla, J. Castagnola, Y. Yamaguchi, J.D. Esko, Cerebral hypoplasia and craniofacial defects in mice lacking heparan sulfate Ndst1 gene function, Development 132 (16) (2005) 3777–3786.
[19] M. Ringvall, J. Ledin, K. Holmborn, T. van Kuppevelt, F. Ellin, I. Eriksson, A.M. Olofsson, L. Kjellen, E. Forsberg, Defective heparan sulfate biosynthesis and neonatal lethality in mice lacking N-deacetylase/N-sulfotransferase-1, J. Biol. Chem. 275 (34) (2000) 25926–25930.
[20] T. Dierker, V. Bachvarova, Y. Krause, J.P. Li, L. Kjellen, D.G. Seidler, A. Vortkamp, Altered heparan sulfate structure in Glce(-/-) mice leads to increased Hedgehog signaling in endochondral bones, Matrix Biol. 49 (2016) 82–92.
[21] T. Mikami, H. Kitagawa, Biosynthesis and function of chondroitin sulfate, Biochim. Biophys. Acta 1830 (10) (2013) 4719–4733.
[22] A. Malmstrom, B. Bartolini, M.A. Thelin, B. Pacheco, M. Maccarana, Iduronic acid in chondroitin/dermatan sulfate: biosynthesis and biological function, J. Histochem. Cytochem. 60 (12) (2012) 916–925.
[23] R.V. Iozzo, L. Schaefer, Proteoglycan form and function: a comprehensive nomenclature of proteoglycans, Matrix Biol. 42 (2015) 11–55.
[24] J. Fukushi, M. Inatani, Y. Yamaguchi, W.B. Stallcup, Expression of NG2 proteoglycan during endochondral and

intramembranous ossification, Dev. Dyn. 228 (1) (2003) 143–148.
[25] Y. Gao, S. Liu, J. Huang, W. Guo, J. Chen, L. Zhang, B. Zhao, J. Peng, A. Wang, Y. Wang, W. Xu, S. Lu, M. Yuan, Q. Guo, The ECM-cell interaction of cartilage extracellular matrix on chondrocytes, Biomed. Res. Int. 2014 (2014) 648459.
[26] A.D. Theocharis, S.S. Skandalis, C. Gialeli, N.K. Karamanos, Extracellular matrix structure, Adv. Drug Deliv. Rev. 97 (2016) 4–27.
[27] M. Cortes, A.T. Baria, N.B. Schwartz, Sulfation of chondroitin sulfate proteoglycans is necessary for proper Indian hedgehog signaling in the developing growth plate, Development 136 (10) (2009) 1697–1706.
[28] S.S. Deepa, Y. Umehara, S. Higashiyama, N. Itoh, K. Sugahara, Specific molecular interactions of oversulfated chondroitin sulfate E with various heparin-binding growth factors. Implications as a physiological binding partner in the brain and other tissues, J. Biol. Chem. 277 (46) (2002) 43707–43716.
[29] E.L. Shipp, L.C. Hsieh-Wilson, Profiling the sulfation specificities of glycosaminoglycan interactions with growth factors and chemotactic proteins using microarrays, Chem. Biol. 14 (2) (2007) 195–208.
[30] J. Kreuger, L. Perez, A.J. Giraldez, S.M. Cohen, Opposing activities of dally-like glypican at high and low levels of wingless morphogen activity, Dev. Cell 7 (4) (2004) 503–512.
[31] L.M. Jenkins, P. Singh, A. Varadaraj, N.Y. Lee, S. Shah, H.V. Flores, K. O'Connell, K. Mythreye, Altering the proteoglycan state of transforming growth factor beta type III receptor (TbetaRIII)/Betaglycan modulates canonical Wnt/beta-catenin signaling, J. Biol. Chem. 291 (49) (2016) 25716–25728.
[32] S. Le Jan, M. Hayashi, Z. Kasza, I. Eriksson, J.R. Bishop, I. Weibrecht, J. Heldin, K. Holmborn, L. Jakobsson, O. Soderberg, D. Spillmann, J.D. Esko, L. Claesson-Welsh, L. Kjellen, J. Kreuger, Functional overlap between chondroitin and heparan sulfate proteoglycans during VEGF-induced sprouting angiogenesis, Arterioscler. Thromb. Vasc. Biol. 32 (5) (2012) 1255–1263.
[33] S. Nadanaka, H. Kinouchi, K. Taniguchi-Morita, J. Tamura, H. Kitagawa, Down-regulation of chondroitin 4-O-sulfotransferase-1 by Wnt signaling triggers diffusion of Wnt-3A, J. Biol. Chem. 286 (6) (2011) 4199–4208.
[34] S. Nadanaka, M. Ishida, M. Ikegami, H. Kitagawa, Chondroitin 4-O-sulfotransferase-1 modulates Wnt-3A signaling through control of E disaccharide expression of chondroitin sulfate, J. Biol. Chem. 283 (40) (2008) 27333–27343.
[35] S. Yamada, M. Busse, M. Ueno, O.G. Kelly, W.C. Skarnes, K. Sugahara, M. Kusche-Gullberg, Embryonic fibroblasts with a gene trap mutation in Ext1 produce short heparan sulfate chains, J. Biol. Chem. 279 (31) (2004) 32134–32141.
[36] G. David, X.M. Bai, B. Van der Schueren, J.J. Cassiman, H. Van den Berghe, Developmental changes in heparan sulfate expression: in situ detection with mAbs, J. Cell Biol. 119 (4) (1992) 961–975.
[37] B. Caterson, Fell-Muir Lecture, chondroitin sulphate glycosaminoglycans: fun for some and confusion for others, Int. J. Exp. Pathol. 93 (1) (2012) 1–10.
[38] A.J. Hayes, C.E. Hughes, B. Caterson, Antibodies and immunohistochemistry in extracellular matrix research, Methods 45 (1) (2008) 10–21.
[39] M. Platzer, J.H. Ozegowski, R.H. Neubert, Quantification of hyaluronan in pharmaceutical formulations using high performance capillary electrophoresis and the modified uronic acid carbazole reaction, J. Pharm. Biomed. Anal. 21 (3) (1999) 491–496.
[40] T. Bitter, H.M. Muir, A modified uronic acid carbazole reaction, Anal. Biochem. 4 (1962) 330–334.
[41] A. Dagalv, A. Lundequist, B. Filipek-Gorniok, T. Dierker, I. Eriksson, L. Kjellen, Heparan sulfate structure: methods to study N-sulfation and Ndst action, Methods Mol. Biol. 1229 (2015) 189–200.
[42] W.C. Lamanna, M.A. Frese, M. Balleininger, T. Dierks, Sulf loss influences N-, 2-O-, and 6-O-sulfation of multiple heparan sulfate proteoglycans and modulates fibroblast growth factor signaling, J. Biol. Chem. 283 (41) (2008) 27724–27735.
[43] A. Dagalv, K. Holmborn, L. Kjellen, M. Abrink, Lowered expression of heparan sulfate/heparin biosynthesis enzyme N-deacetylase/n-sulfotransferase 1 results in increased sulfation of mast cell heparin, J. Biol. Chem. 286 (52) (2011) 44433–44440.
[44] A. Deligny, T. Dierker, A. Dagalv, A. Lundequist, I. Eriksson, A.V. Nairn, K.W. Moremen, C.L. Merry, L. Kjellen, NDST2 (N-deacetylase/N-sulfotransferase-2) enzyme regulates heparan sulfate chain length, J. Biol. Chem. 291 (36) (2016) 18600–18607.
[45] S.R. Pallerla, R. Lawrence, L. Lewejohann, Y. Pan, T. Fischer, U. Schlomann, X. Zhang, J.D. Esko, K. Grobe, Altered heparan sulfate structure in mice with deleted NDST3 gene function, J. Biol. Chem. 283 (24) (2008) 16885–16894.
[46] C.L. Merry, S.L. Bullock, D.C. Swan, A.C. Backen, M. Lyon, R.S. Beddington, V.A. Wilson, J.T. Gallagher, The molecular phenotype of heparan sulfate in the Hs2st-/- mutant mouse, J. Biol. Chem. 276 (38) (2001) 35429–35434.
[47] K. Lidholt, J.L. Weinke, C.S. Kiser, F.N. Lugemwa, K.J. Bame, S. Cheifetz, J. Massague, U. Lindahl, J.D. Esko, A single mutation affects both N-acetylglucosaminyltransferase and glucuronosyltransferase activities in a Chinese hamster ovary cell mutant defective in heparan sulfate biosynthesis, Proc. Natl. Acad. Sci. USA 89 (6) (1992) 2267–2271.
[48] K. Holmborn, J. Habicher, Z. Kasza, A.S. Eriksson, B. Filipek-Gorniok, S. Gopal, J.R. Couchman, P.E. Ahlberg, M. Wiweger, D. Spillmann, J. Kreuger, J. Ledin, On the roles and regulation of chondroitin sulfate and heparan sulfate in zebrafish pharyngeal cartilage morphogenesis, J. Biol. Chem. 287 (40) (2012) 33905–33916.
[49] J. Huegel, C. Mundy, F. Sgariglia, P. Nygren, P.C. Billings, Y. Yamaguchi, E. Koyama, M. Pacifici, Perichondrium phenotype and border function are regulated by Ext1 and heparan sulfate in developing long bones: a mechanism likely deranged in hereditary multiple exostoses, Dev. Biol. 377 (1) (2013) 100–112.
[50] S. Gulberti, V. Lattard, M. Fondeur, J.C. Jacquinet, G. Mulliert, P. Netter, J. Magdalou, M. Ouzzine, S. Fournel-Gigleux, Modifications of the glycosaminoglycan-linkage region of proteoglycans: phosphorylation and sulfation determine the activity of the human beta1,4-galactosyltransferase 7 and beta1,3-glucuronosyltransferase I, Sci. World J. 5 (2005) 510–514.
[51] S. Gulberti, J.C. Jacquinet, M. Chabel, N. Ramalanjaona, J. Magdalou, P. Netter, M.W. Coughtrie, M. Ouzzine, S. Fournel-Gigleux, Chondroitin sulfate N-acetylgalactosaminyltransferase-1 (CSGalNAcT-1) involved in chondroitin sulfate initiation: impact of sulfation on activity and specificity, Glycobiology 22 (4) (2012) 561–571.
[52] X. Bai, G. Wei, A. Sinha, J.D. Esko, Chinese hamster ovary cell mutants defective in glycosaminoglycan assembly and glucuronosyltransferase I, J. Biol. Chem. 274 (19) (1999) 13017–13024.

[53] K.I. Stanford, L. Wang, J. Castagnola, D. Song, J.R. Bishop, J.R. Brown, R. Lawrence, X. Bai, H. Habuchi, M. Tanaka, W.V. Cardoso, K. Kimata, J.D. Esko, Heparan sulfate 2-O-sulfotransferase is required for triglyceride-rich lipoprotein clearance, J. Biol. Chem. 285 (1) (2010) 286–294.

[54] M. Logan, J.F. Martin, A. Nagy, C. Lobe, E.N. Olson, C.J. Tabin, Expression of Cre recombinase in the developing mouse limb bud driven by a Prxl enhancer, Genesis 33 (2) (2002) 77–80.

[55] J. Schindelin, I. Arganda-Carreras, E. Frise, V. Kaynig, M. Longair, T. Pietzsch, S. Preibisch, C. Rueden, S. Saalfeld, B. Schmid, J.Y. Tinevez, D.J. White, V. Hartenstein, K. Eliceiri, P. Tomancak, A. Cardona, Fiji: an open-source platform for biological-image analysis, Nat. Methods 9 (7) (2012) 676–682.

[56] R.A. McCloy, S. Rogers, C.E. Caldon, T. Lorca, A. Castro, A. Burgess, Partial inhibition of Cdk1 in G2 phase overrides the SAC and decouples mitotic events, Cell Cycle 13 (9) (2014) 1400–1412.

[57] T.D. Schmittgen, K.J. Livak, Analyzing real-time PCR data by the comparative C(T) method, Nat. Protoc. 3 (6) (2008) 1101–1108.

[58] K.I. Stanford, J.R. Bishop, E.M. Foley, J.C. Gonzales, I.R. Niesman, J.L. Witztum, J.D. Esko, Syndecan-1 is the primary heparan sulfate proteoglycan mediating hepatic clearance of triglyceride-rich lipoproteins in mice, J. Clin. Investig. 119 (11) (2009) 3236–3245.

[59] J. Riesenfeld, M. Hook, U. Lindahl, Biosynthesis of heparin. Concerted action of early polymer-modification reactions, J. Biol. Chem. 257 (1) (1982) 421–425.

[60] J. Ledin, W. Staatz, J.P. Li, M. Gotte, S. Selleck, L. Kjellen, D. Spillmann, Heparan sulfate structure in mice with genetically modified heparan sulfate production, J. Biol. Chem. 279 (41) (2004) 42732–42741.

[61] R. Lawrence, H. Lu, R.D. Rosenberg, J.D. Esko, L. Zhang, Disaccharide structure code for the easy representation of constituent oligosaccharides from glycosaminoglycans, Nat. Methods 5 (4) (2008) 291–292.